Opportunities for Adaptation and Learning in Dynamically Stable Legged Robots

I. Poulakakis[1], J. Smith[1], E. Papadopoulos[2] and M. Buehler[1]

[1]Ambulatory Robotics Laboratory, http://www.mcgill.cim.ca/~arlweb
Centre for Intelligent Machines, McGill University, Montreal, CANADA
[2]Department of Mechanical Engineering, NTU Athens, GREECE

ABSTRACT

This paper addresses the control and aspects of modeling for Scout II, an autonomous four-legged robot with only one actuator per compliant leg. The running controller requires minimal task level feedback, yet achieves reliable, efficient and fast running up to 1.2 m/s - apparently complex dynamically dexterous tasks may be controlled via simple control laws. We demonstrate the need to model the actuators and the power source of the robot system carefully in order to obtain experimentally valid models for simulation and analysis. The availability of validated models and the small number of controller parameters, makes this type of robot a good candidate for further performance improvements based on adaptation and learning.

1. Introduction

We have pursued an agenda of low mechanical complexity in our Scout I and II quadruped robots, in order to decrease cost and increase reliability. In contrast, most existing four- or eight-legged robots are designed for statically stable operation – stability is assured by keeping the machine's center of mass above the polygon formed by the supporting feet. While this is the safest mode of locomotion, it comes at the cost of mobility and speed. Furthermore it requires a high mechanical complexity of three degrees of freedom per leg to provide body support during motion.

We have shown in [5,6] that dynamic walking, turning and step climbing can be achieved with a quadruped with stiff legs and only one hip actuator per leg. Equipped with only an additional compliant prismatic joint per leg, our Scout II robot is able to run with a bounding gait (Fig. 1). We will show that this type of dynamic running gait is possible with a very simple control strategy. Open loop control, simply positioning the legs at a fixed angle during flight, and commanding a fixed leg sweep angular velocity during stance results in a stable bounding gait. To our knowledge, Scout II is the first autonomous quadruped that achieves compliant running, features the simplest running control algorithm, and the simplest mechanical design to date.

We also address two subjects that have not yet received the attention they require in order to advance the state of the art in autonomous, dynamically stable legged locomotion – experimentally validated models and energetics. Autonomous legged robots operate at the limits of their actuators, and require a model of the actuator dynamics and their interaction with the power source. We show that for Scout II, and likely for most other robots in its class, ignoring these issues results in inaccurate models. And without valid models, model based adaptation and learning methods are doomed to fail when ported to the experimental platform.

In addition, energy efficiency and autonomy are essential for mobile robots. In order to characterize the energetics of Scout II, we document the running efficiency as a function of speed, based on both the mechanical actuator output power, and the total electrical input power.

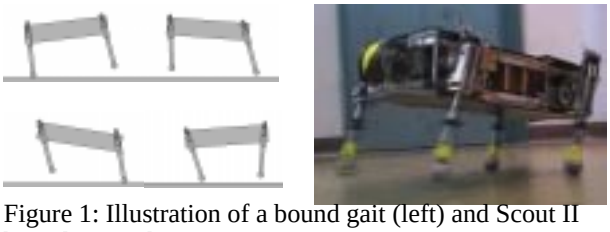

Figure 1: Illustration of a bound gait (left) and Scout II bounding (right).

Ongoing research addresses compliant walking, rough terrain locomotion and dynamic stair climbing with Scout II, while another paper [9] demonstrated a trotting (walking) gait, based on additional passive, but lockable, knee joints and non-compliant legs. The approach of using only one actuated degree of freedom per leg, compliant legs, and task-space open loop controllers has recently also been applied successfully to a dynamic hexaped, RHex [14]. This biologically inspired robot has the added advantage of a low center of mass and sprawled posture and is able to negotiate rough terrain at roughly one body length per second.

Only few cases of quadruped running robots have been reported in the literature. About 15 years ago, Raibert [13] set the stage with his groundbreaking work on a dynamically stable quadruped, which implemented his three-part controller, via generalizations of the virtual leg idea. The robot featured three hydraulically actuated and one passive prismatic DOF per leg. The robot was able to trot, pace and bound, with smooth transitions between these gaits. Furusho et al. [7] implemented a bounding gait on the Scamper robot. The controller divided one complete running cycle into eight states and switched the two joints per leg between free rotation, position control and velocity control.

Akiyama and Kimura [3] implemented a bounding gait in the Patrush robot. Each three DOF leg featured an actuated hip and knee, and an unactuated, compliant foot joint. Their neural oscillator based controller was motivated by Matsuoka [11], which also underlies the control of the simulated planar biped of Taga et al [15]. An additional reflex network was added to the neural oscillator to achieve the stability and robustness necessary for experimental success.

2. Scout II Design and Modeling

Scout II has been designed from the ground up for autonomous operation: The two hip assemblies contain the actuators and batteries, and the body houses all computing, interfacing and power distribution. The mechanical design of Scout II (Fig. 2) is an exercise in simplicity. Besides its modular design, the most striking feature is the fact that it uses a single actuator per leg – the hip joint provides leg rotation in the sagittal plane. Each leg assembly consists of a lower and an upper leg, connected via a spring to form a compliant prismatic joint. Thus each leg has two degrees of freedom, one actuated hip and one unactuated linear spring.

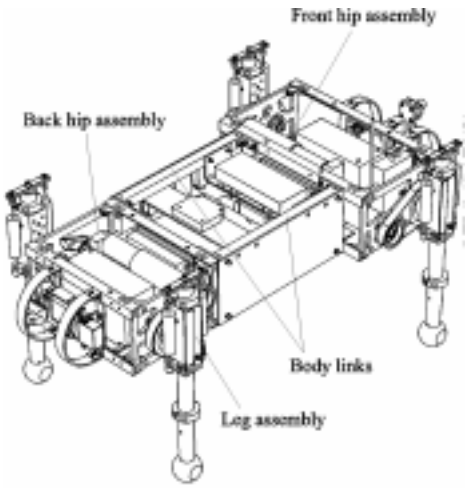

Figure 2. Scout II

Scout II in planar motion is modeled in WorkingModel 2D [10] as a five-body kinematic chain, shown in Fig. 3. A linear spring and damper system models the leg compliance during stance phase. Since each of the two legs can be in stance or flight, there are four robot states: front flight-back stance, front stance-back flight, double flight, and double stance.

Figure 3. Scout II sagittal diagram

3. Bounding Controller

Scout II is an under-actuated, highly nonlinear, intermittent dynamical system. Despite this complexity, we found that simple control laws can stabilize periodic motions, resulting in robust and fast running. Surprisingly, the controllers do not require task level feedback like forward velocity, or body angle. What is more, there seem to exist many such simple stabilizing controllers – in [16] three variations are introduced. It is remarkable that the significant controller differences have relatively minor effects on bounding performance! For this reason and for brevity we shall describe one of these controllers here.

The controller is based on two individual, independent leg controllers, without a notion of overall body state. The front and back legs each detect two leg states - stance (touching ground) and flight (otherwise), which are separated by touchdown and lift-off events. There is no actively controlled coupling between the fore and hind legs – the resulting bounding motion is purely the result of the controller interaction through the multi-body dynamic system. During flight, the controller servos the flight leg to a desired touchdown hip angle, ϕ_{td} then sweeps the leg during stance until a sweep limit, ϕ_{sl} is reached**.** In stance phase, a constant torque of 35 Nm is commanded at the hip until the sweep limit is reached. Then a PD controller controls the hip angle at the sweep limit angle. The tracking gains are shown, together with the controller parameter settings, in Table 1. Even though we show only the results for one of several controllers implemented, experimental performance for all of them is very similar – resulting in stable and robust bounding, at top speeds between 0.9 and 1.2 m/s.

Table 1: Controller parameters and PD gains

$\phi_{td}(^o)$	20
$\phi_{sl}(^o)$	0
$k_{p,s}$ *and* $k_{p,f}$ $(Nm/^o)$	35
$k_{d,s}$ *and* $k_{d,f}$ $(Nm/^o s)$	0.15

Figures 7 and 8 compare the body angle trajectories and torque profiles between simulations and experiment. The stride frequency as well as the body oscillation amplitude matches well. Also on the torque

level, the traces are qualitatively similar, but there are still many details which differ. Some of these are likely due to inaccurately modeled ground-toe friction, and unmodeled compliance in the leg. These remaining differences are still the subject of ongoing work.

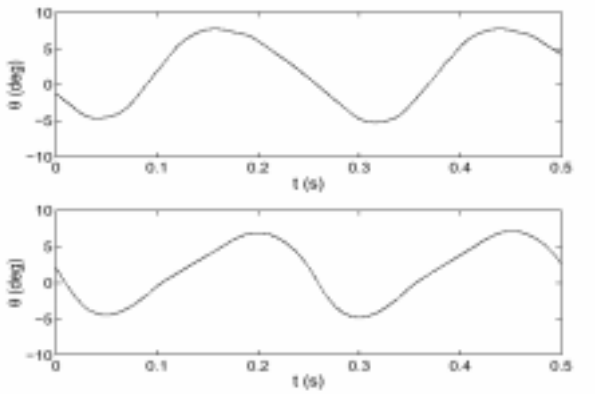

Figure 7: Body angle. Experiment (top), simulation (bottom).

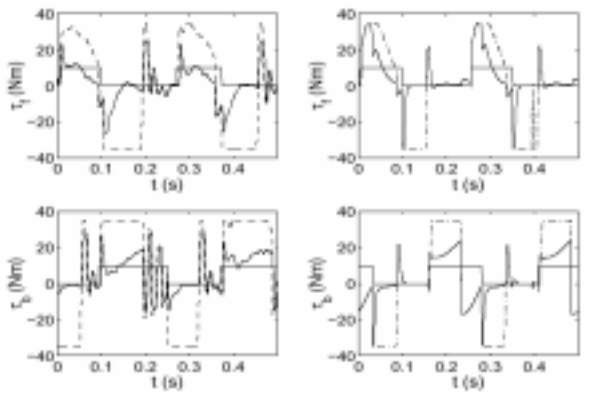

Figure 8: Front (top) and back (bottom) actuator torques. Commanded torques (dash) vs. measured torques (solid). Experiments (left) vs. simulation (right). The solid square wave denotes the leg state: stance (high) and flight (low).

4. Actuator and Power Source Modeling

It is well known that dynamically stable legged robots are complex dynamical systems with intermittent variable structure dynamics, fewer actuators than motion degrees of freedom, impacts, unilateral toe-ground constraints, and limited ability to apply tangential ground forces due to slip. These qualities greatly complicate modeling and usually prevent the application of classical control synthesis. In this section we demonstrate two additional modeling components which are dominant on our Scout II robot, and which are likely to be significant in dynamically stable legged robots in general – actuator and power source modeling.

Designing an autonomous dynamically stable robot is a formidable system design challenge. For example, the robot weight should be kept to a minimum, yet the actuators have to be capable not only to support the robot weight, but also to impart significant accelerations to the body, and support large dynamic loads. As a result, the actuators will typically operate at their limits, characterized by their torque-speed curve. While this curve is well known, it is typically not taken into account in robot modeling and control. As we will see below, ignoring this constraint will result in large differences between commanded and actually achieved torques.

The torque speed limitation of an electrical actuator can be characterized in the first quadrant by

$$\tau \le \min(\frac{K}{R_A}(V_T - K\omega), \tau_{\max})$$

where K is the motor torque constant (SI units), R_A is the motor armature resistance, ω is the motor speed, V_T is the motor terminal voltage, and $\tau_{\max}$ is the fixed torque limit imposed by the motor amplifiers' current constraint. Figure 4 below shows the large difference between desired torques (top plots), and actually achievable torques (lower plots), for a fixed power supply or battery voltage.mobile manipulator.

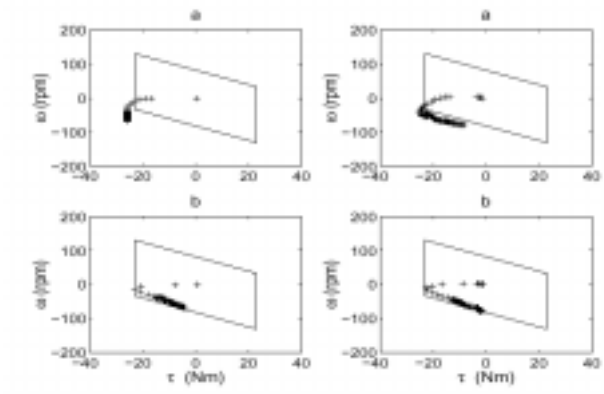

Figure 4: Experimental results. Torque speed plot for the back (left), and front legs (right) actuators. Top plot shows commanded torques and bottom plots show actually achievable torques.

Since electrically actuated autonomous robots can draw significant peak power and operate from non-ideal voltage sources, the variation of the supply voltage as a function of the total load current must be considered. Fig. 5 shows the drastic supply voltage fluctuations, and that a simple battery model, consisting of a fixed internal voltage source in series with an internal resistance results in a very good match between the measured and modeled supply voltage.

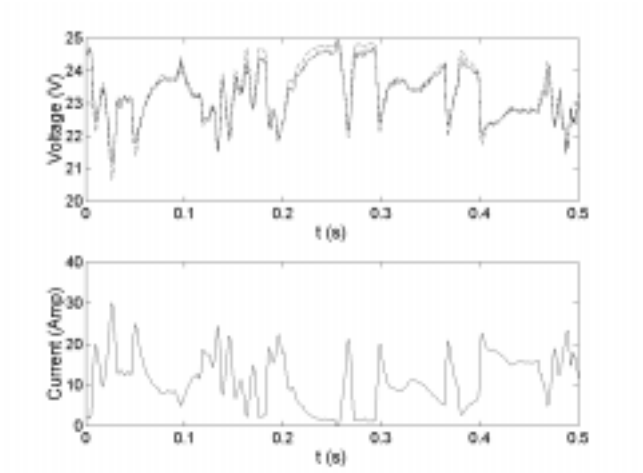

Figure 5: Measured battery voltage fluctuations (top, solid) as a function of measured battery current (bottom). The top graph shows both the measured battery voltage (solid) and the battery voltage estimation (dash) based on an internal (nominal) battery voltage of 25 Volts in series with an internal battery resistance of 0.14 Ohms.

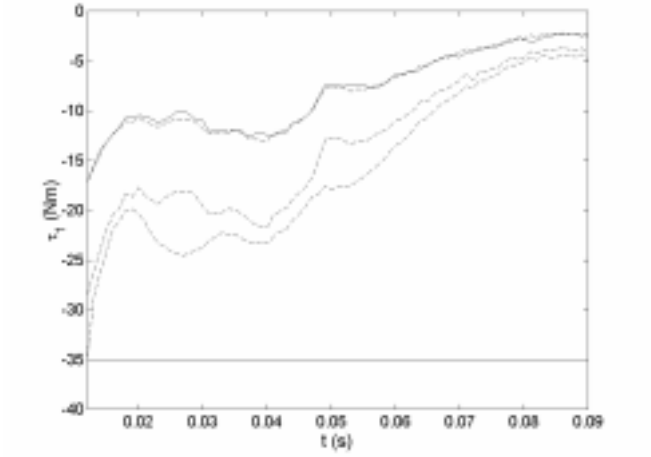

Figure 6: Torque profiles during one stance phase. Data traces from bottom to top: Commanded torque of –35 Nm from the controller (solid), maximum achievable torque based on torque speed curve with fixed 24 V battery voltage (dashed), maximum achievable torque based on battery voltage model; additional loop gain fix due to amplifier gain modeling error; measured motor torque (solid).

Fig. 6 demonstrates both the large discrepancy between desired (upper solid line) and achievable motor torques (lower solid line) and the accuracy of the combined actuator/power model (shown by the closely matching solid and dashed lines). It is interesting to point out that, due to the multitude of dynamic, actuation, and power constraints, it is nearly impossible to control either torque or leg angular velocity during stance arbitrarily. The controller can only affect the system dynamics during stance in a limited fashion. For this reason it is important that the robot's passive (unforced) dynamics be as close as possible to the desired motion. Indeed, this is likely one of the reasons for the successful operation of Scout II. In addition, the actuation constraints during stance suggest the use of the leg touchdown angle (which is easily controlled during flight) as a dominant control input. As shown in the previous section, this is one of the control parameters in our bounding controller.

5. Energetics

For mobile robots to be of practical utility, they need to be energy efficient and able to operate in a power-autonomous fashion for extended periods of time. Thus, energy efficiency is an important performance measure of mobile robots. An increasingly accepted measure of energy efficiency is the 'specific resistance' – a measure proposed originally by Gabrielli and von Karman [8] in 1950,

$$\varepsilon(v) = \frac{P(v)}{mgv}$$

where P is the average power expenditure, m is the mass of the vehicle, g is the gravitational acceleration, and v is the vehicle forward speed. Since many vehicle specific resistances quoted in the literature are based on the average mechanical output power of the actuators, we have calculated this figure as a function of speed (Fig. 10). Even though energy efficiency has so far not been optimized, Scout II at top speed already achieves a low specific resistance of 0.32. This value places Scout II among the most energy efficient running robots, in terms of mechanical power. This is only slightly higher than the (lowest published running robot efficiency) 0.22 value for the ARL Monopod II [2], but still lower than any other running robot.

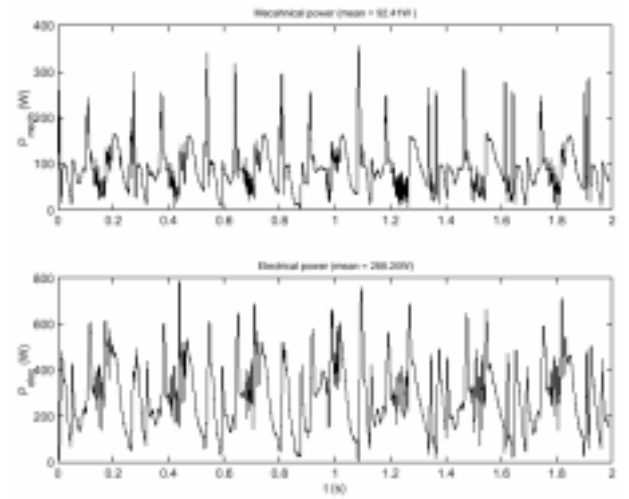

Fig. 9: Mechanical (top) and total electrical (bottom) power consumption at 1.15 m/s

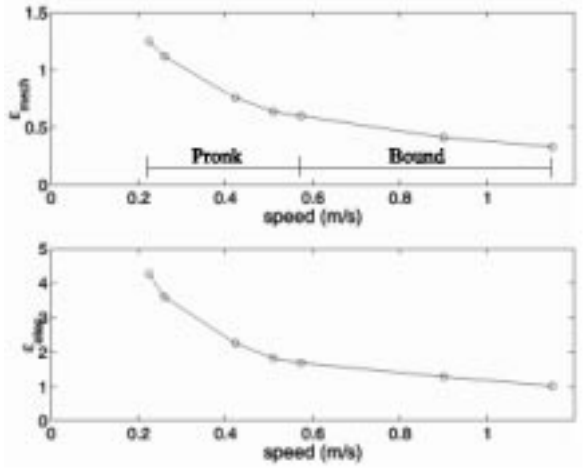

Fig. 10: Specific resistance as a function of forward speed based on mechanical (top) and total electrical (bottom) power consumption.

The specific resistance based on mechanical output power has drawbacks, since it does not take the actuator efficiency or the power consumption of the entire system into account. Both of these effects can have a dramatic negative influence on runtime. Therefore, a more useful measure of energy efficiency, is the specific resistance based on total power consumption. For a system with a battery as the main power source, this is the total average product of battery current and voltage. For Scout II, this value is approximately 1.0, three times the specific resistance based on mechanical power. We suspect that this value is still low for a running robot, and that even the large difference between electrical and mechanical power is normal; however, little comparable data is available from other robots to date, and we hope that the reporting of mechanical output power and total electrical input power will become standard practice for mobile robots in the future.

6. Scout I

An even simpler example for a dynamically stable robot is Scout I, the precursor to Scout II. It lacks the linear leg compliance of Scout II (Fig. 11) and relies on inelastic font and back leg-ground impacts and the resulting momentum transfer to maintain a "bounding walk" [5,6].

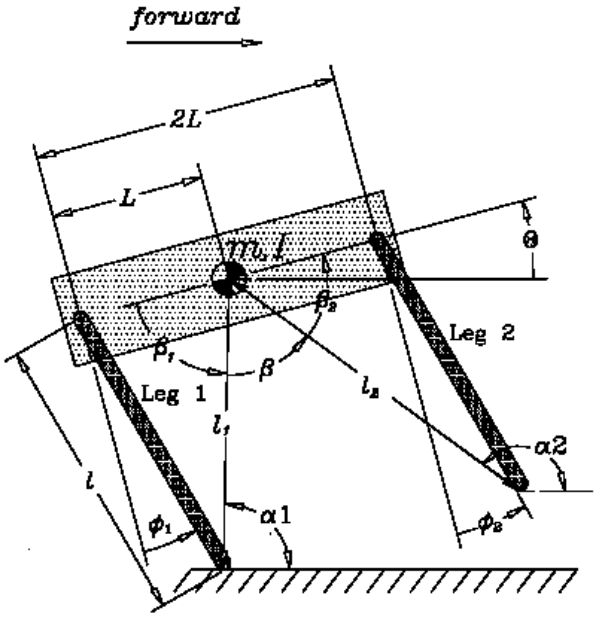

Fig. 11: Scout I model in the sagittal plane.

Stable open loop walking was achieved, as shown in Fig. 12, by maintaining the front legs at a fixed angle, and sweeping the back legs at a fixed desired hip speed as long as they are on the ground, and starting from a commanded touchdown leg angle. Therefore, this "ramp controller" is parametrized by only two parameters, the back leg touchdown angle and the back leg angular sweep speed. Thus, if only forward walking is required, the quadruped robot can be actuated via a single motor driving both back legs in unison, making it arguable the simplest possible (actuated) dynamically stable walking robot possible. This same simplicity also makes it an ideal candidate for adaptation and learning as outlined in section 7.

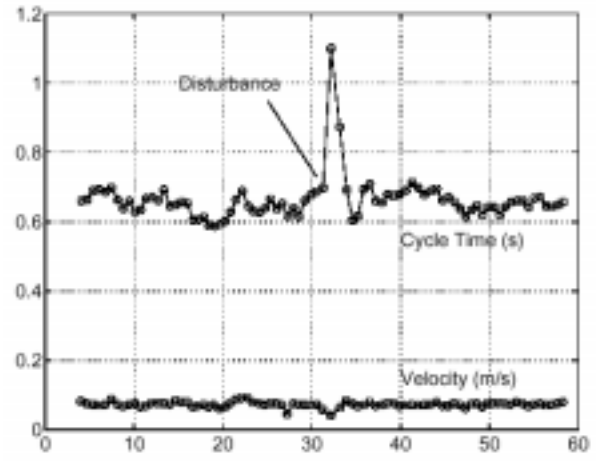

Fig. 12: Scout I stable experimental performance with open loop ramp controller (from [5]). Due to a lack of body angle measurements on this robot, the more easily

accessible cycle time is shown to document walking stability and robustness to disturbance.

7. Opportunities for Adaptation and Learning

Our work has so far focused on three components. First, simple mechanical robot designs that admit passive dynamics close to the desired locomotion tasks. Second, experimentally validated dynamic models as a basis for controller development and future model-based control. And finally, the synthesis of the most elementary controllers, using as little feedback as possible, to achieve fundamental walking and running tasks. Due to the complexity of discrete dynamical models on a Poincaré section, and our inability to construct their closed form expressions in the first place, our controller synthesis so far is based on intuition and iterative simulations and experiments.

Here are interesting applications for adaptation and learning. Even for the running controller parameterization presented, it is unlikely that our choice is optimal with respect to stability, robustness, and energy efficiency for any particular speed. And currently we only have a few parameter selections corresponding to selected forward speeds. A velocity dependent controller parameterization that maximizes our performance criterion would be ideal. Further gains could be achieved by introducing a richer controller parameter set (e.g. polynomial stance torque trajectories), or by eliminating a parametric controller model altogether, and generating torque profiles numerically.

8. Conclusion

In this paper we presented an algorithm that controls compliant bounding for a quadruped robot with only one actuator per leg. The algorithm was derived and tested in simulations, which incorporated a validated model for the actuators and the power source. Experimental runs showed good correspondence with the simulations. Experimental data was used to show a low specific resistance of 0.32 when based on mechanical power and of 1.0 when based on total electrical power.

9. Acknowledgments

This project was supported in part by IRIS, a Federal Network of Centers of Excellence and the Natural Sciences and Engineering Research Council of Canada (NSERC). We also acknowledge the contributions of S. Talebi and K. Yamazaki to this work, and the generous and talented help of G. Hawker, M. de Lasa, D. Campbell, D. McMordie, E. Moore, and S. Obaid. Portions of this work have been reported earlier in [17].

References

[1] M. Ahmadi and M. Buehler, "Stable Control of a Simulated One-Legged Running Robot with Hip and Leg Compliance," IEEE Trans. Robotics and Automation, 13(1):96-104, Feb 1997.

[2] M. Ahmadi and M. Buehler, "The ARL Monopod II Running Robot: Control and Energetics," IEEE Int. Conf. Robotics and Automation, p. 1689-1694, May 1999.

[3] S. Akiyama and H. Kimura, "Dynamic quadruped walk using neural oscillators - Realization of pace and trot," 13. Ann. Conf. RSJ, p. 227 - 228, 1995.

[4] G. N. Boone and J. K. Hodgins. "Reflexive Responses to Slipping in Bipedal Running Robots," IEEE Int. Conf. Intelligent Robots and Systems, p. 158–164, May 1995.

[5] M. Buehler et al, "Scout: A simple quadruped that walks, climbs and runs," IEEE Int. Conf. Robotics and Automation, p. 1701-1712, May 1998.

[6] M. Buehler et al, "Stable Open Loop Walking in Quadruped Robots with Stick Legs," IEEE Int. Conf. Robotics and Automation, p. 2348-2353, May 1999.

[7] J. Furusho et al, "Realization of Bounce Gait in a Quadruped Robot with Articular-Joint-Type Legs," IEEE Int. Conf. Robotics and Automation, p. 697-702, May 1995.

[8] G. Gabrielli and T. H. von Karman, “What price speed?” Mechanical Engineering, vol. 72, no. 10, 1950.

[9] G. Hawker and M. Buehler, "Quadruped Trotting with Passive Knees," IEEE Int. Conf. Robotics and Automation, April 2000.

[10] Knowledge Revolution. *Working Model 2D User’s Guide*. San Mateo, CA, 1996.

[11] K. Matsuoka, "Sustained oscillations generated by mutually inhibiting neurons with adaptation," Biol. Cybernetics, 52:367-376, 1985.

[12] D. Papadopoulos, "Stable Running for a Quadruped Robot with Compliant Legs," M. Eng. Thesis, McGill University, 2000.

[13] M. H. Raibert. *Legged Robots That Balance*. MIT Press, Cambridge, MA, 1986.

[14] U. Saranli, M. Buehler and D. E. Koditschek, "Design, Modeling and Preliminary Control of a Compliant Hexapod Robot," IEEE Int. Conf. Robotics and Automation, April 2000.

[15] G. Taga, Y. Yamaguchi, and H. Shimizu, "Self-organized control of bipedal locomotion by neural oscillators in unpredictable environment," Biol. Cybernetics, Vol. 65, p. 147 - 159, 1991.

[16] S. Talebi, “Compliant Running and Step Climbing of the Scout II Platform”, M. Eng. Thesis, McGill University, 2000.

[17] S. Talebi et al., “Quadruped Robot Running with a Bounding Gait”, Int. Symp. Experimental Robotics, Dec. 2000.